metals

MDPI

Article

Electroplating Nickel Coatings on Foam Nickel for Sand Control Screens

Wenbo Wang [1,†], Xinyang Luo [1,†], Zhen Pei [1], Shengchi Bai [2], Wen Wen [2], Huidi Yu [2], Xiaoqi Wang [2,*] and Xingzhong Guo [1,3,*]

[1] State Key Laboratory of Silicon and Advanced Semiconductor Materials, School of Materials Science and Engineering, Zhejiang University, Hangzhou 310058, China; wbwang01@zju.edu.cn (W.W.); 3220106310@zju.edu.cn (X.L.); 12426004@zju.edu.cn (Z.P.)
[2] Research Institute of Petroleum Exploration & Development of China National Petroleum Corporation (RIPED), Beijing 100083, China; baisc21@petrochina.com.cn (S.B.); wenwen21@petrochina.com.cn (W.W.); yuhd21@petrochina.com.cn (H.Y.)
[3] ZJU-Hangzhou Global Scientific and Technological Innovation Center, Hangzhou 311200, China
* Correspondence: wangxq07@petrochina.com.cn (X.W.); msewj01@zju.edu.cn (X.G.)
† These authors contributed equally to this work.

Abstract

Nickel foam filtration layers used in sand control screens for petroleum extraction often suffer from insufficient mechanical strength and poor corrosion resistance and wear resistance. In this work, a two-stage electroplating strategy using the same metal was employed to construct hierarchical nickel coatings on nickel foam substrates. The effects of key process parameters, including electroplating time, temperature, and pretreatment, on the microstructure, mechanical properties, electrochemical corrosion behavior, and tribological performance of the coatings were systematically investigated. Electroplating time was found to directly regulate grain size and coating uniformity, while electroplating temperature significantly influenced nickel deposition behavior and electrolyte stability. In addition, UV pretreatment markedly improved the brightness and homogeneity of the deposited layers. Under optimized conditions (UV pretreatment for 10 min, electroplating at 60 °C for 8 min), a dense and uniform nickel coating with a well-ordered crystalline structure was obtained, leading to significantly enhanced hardness, wear resistance, and corrosion resistance. This study presents a practical and highly reliable approach for fabricating high-performance nickel-based coatings on nickel foam filter layers. Anticipated for application in the oil extraction industry, this method is set to enhance the performance of foam metal sand control layers.

Keywords: sand control screen; nickel foam; electroplating; crystalline nickel coating

Check for updates

Academic Editor: Nebojša Nikolić

Received: 4 February 2026
Revised: 21 February 2026
Accepted: 24 February 2026
Published: 26 February 2026

Copyright: © 2026 by the authors. Licensee MDPI, Basel, Switzerland. This article is an open access article distributed under the terms and conditions of the Creative Commons Attribution (CC BY) license.

1. Introduction

Sand production in oil wells represents a critical technical bottleneck, which severely constrains efficient oilfield development. This phenomenon not only causes reservoir structure damage and formation spalling to jeopardize production safety, but also accelerates the wear and clogging of oil extraction equipment to significantly compromise production stability. In the petroleum extraction systems, sand filtration serves as a core process, whose technological sophistication directly determines crude oil quality and the advancement level of the energy industry [1,2]. Although metal filter screens are widely adopted in petroleum filtration applications, conventional materials under high-intensity extraction

conditions exhibit inherent limitations, such as rapid corrosion rates and fatigue fractures. These deficiencies lead to reduced sand control efficiency and diminished crude oil purity, substantially hindering improvements in both extraction efficiency and economic returns [3–5].

As an indispensable surface treatment process in modern manufacturing, the electroplating technology plays a pivotal role in enhancing material performance [6,7], which can prepare metallic coatings on substrate surfaces to significantly improve the wear resistance, corrosion resistance, and mechanical strength of components (e.g., Ni, Ni-SiC, Ni-Al_2O_3, and Ni-BN coatings) [8–11]. The electroplating technology has wide application in different industries. For instance, in the electronic manufacturing, electroplating technology is widely employed for the fabrication of printed circuit board (PCB) traces and component interconnections [12]. To effectively prevent the corrosion of steel equipment, the Zn/Ni-Zn coating with excellent corrosion resistance has been widely used in fields such as automotive and aerospace [13]. Among various metallic coatings, nickel plating has garnered significant attention due to its superior comprehensive properties. Nickel coatings exhibit high hardness and tensile strength and exceptional wear resistance, which substantially prolongs the service life of workpieces. Seyed Mohammad Jesmani et al. reported that the uncoated copper substrate initially had a hardness of approximately 72 HV, comparable to that of nickel foam. The hardness of the copper substrate increased to about 136 HV after additive-free nickel electrodeposition on its surface. With an appropriate amount of additives, the hardness could be further enhanced to 307 HV, demonstrating a significant improvement in material hardness [14]. This value is significantly higher than the average hardness of nickel foam. Moreover, the Archard equation indicates that the wear rate of a coating is inversely proportional to its hardness, suggesting that high-hardness nickel coatings exhibit superior wear resistance [15]. Furthermore, nickel coatings maintain excellent chemical stability even under harsh environmental conditions. Yuttanant Boonyongmaneerat et al. reported that pure Ni coatings exhibit superior corrosion resistance to biodiesel and its vapor phase compared to Ni-W alloy coatings [11]. Combined with their dense and uniform microstructure, these characteristics render nickel plating an indispensable surface treatment solution for industrial applications [16–19].

Conventional electroplating processes predominantly employ dissimilar metal combinations between coating and substrate, while research on the same metals between coatings and substrates remains relatively scarce. In the nickel foam-based composites, the electroplating nickel coating offers distinct advantages. During the plating process, factors such as the surface condition of the substrate, moisture in the air, the size of the workpiece, and the presence of impurity gases can lead to the formation of pores on the surface of the nickel coating. These pores can give rise to microscopic corrosion cells during service, and since the nickel coating acts as the cathodic layer, it accelerates the corrosion of the substrate, ultimately leading to coating failure [20,21]. Wu et al. reported that, compared with single-layer coatings, multilayer nickel-based coatings exhibit a longer service life and superior corrosion resistance. Electrodeposition provides excellent controllability over coating thickness and composition under mild processing conditions [22]. The resulting coatings typically exhibit high uniformity, strong interfacial adhesion, and improved corrosion resistance, making the technique suitable for industrial applications [23]. Therefore, the present study focuses on the electrodeposition of nickel using a two-step plating method. It eliminates the risk of galvanic corrosion associated with dissimilar metal contact, enhances material property consistency, and potentially achieves superior interfacial bonding strength. Currently, a large number of studies have focused on the preparation methods of nickel coatings on other metal materials. However, there is a relative lack of research

on enhancing the mechanical and chemical properties of nickel foam by means of nickel coatings [24–29].

In this work, we employed two-stage electroplating process to fabricate nickel coatings on the nickel foam, and systematically investigated the influence mechanisms of electroplating time, temperature and pretreatment processes on the surface morphology and microstructure of nickel coatings. Particular emphasis was placed on examining the mechanical properties, wear resistance and electrochemical performance of nickel-plated nickel foam. Advanced characterization techniques were utilized, in conjunction with tribological wear tests and electrochemical measurements, to comprehensively evaluate the performance characteristics of nickel-plated nickel foam under different process parameters.

2. Specimen Preparation and Characterization Methods

2.1. Electroplating Solution Preparation

Two electroplating bath systems were employed in this study, and the preparation procedures were as follows. For the primary plating bath used in the first-stage electroplating, the electrolyte consisted of 25 g L^{-1} $NiSO_4 \cdot 6H_2O$ (Analytical reagent, AR, Macklin Scientific, Shanghai, China), 10 g L^{-1} $NiCl_2 \cdot 6H_2O$ (AR, Aladdin Scientific, Shanghai, China), 10 g L^{-1} $C_6H_5Na_3O_7$ (AR, Aladdin Scientific, Shanghai, China), and 2 g L^{-1} H_3BO_3 (AR, Aladdin Scientific, Shanghai, China) dissolved in deionized water. In addition, 8 g L^{-1} $C_{12}H_{25}SO_4Na$ (AR, Aladdin Scientific, Shanghai, China) was added as a wetting agent. The pH of the solution was adjusted to 1.5 ± 0.1 using a 10 wt% H_2SO_4 (Aladdin Scientific, Shanghai, China) solution. For the secondary plating bath used in the second-stage electroplating, the electrolyte was composed of 37.5 g L^{-1} $NiSO_4 \cdot 6H_2O$ (AR, Aladdin Scientific, Shanghai, China), 12.5 g L^{-1} $NiCl_2 \cdot 6H_2O$ (AR, Aladdin Scientific, Shanghai, China), and 1.25 g L^{-1} H_3BO_3 (AR, Aladdin Scientific, Shanghai, China). Subsequently, 12.5 g L^{-1} $C_7H_4NNaO_3S$ (Aladdin Scientific, Shanghai, China) was added as a brightener, and the pH value was adjusted to 5.0 ± 0.2 using a 5 wt% NaOH (Aladdin Scientific, Shanghai, China) solution.

2.2. Substrate Pretreatment and Electroplating Process

The substrates were 2 mm thick nickel foam (Debye Scientific, Shanghai, China) (13 mm × 50 mm, 99.9% purity, 95% porosity) and 1 mm thick 304 stainless steel sheets (Macklin Scientific, Shanghai, China) (13 mm × 50 mm). The pretreatment procedure included alkaline degreasing, activation, rinsing and drying. The substrates were immersed in an alkaline solution containing 10 g L^{-1} NaOH, 15 g L^{-1} Na_2CO_3 (AR, Aladdin Scientific, Shanghai, China) and 20 g L^{-1} Na_3PO_4 (AR, Aladdin Scientific, Shanghai, China), and were ultrasonic-cleaned at 60 °C for 10 min. Then, the alkaline degreased substrates were activated with 10% (v/v) HCl (AR, Aladdin Scientific, Shanghai, China) solution at room temperature for 30 s. After that, the activated substrates were ultrasonic-cleaned in deionized water for 3 min and repeated three times. Finally, the substrates were rinsed with anhydrous ethanol and drying for further experiments.

Then, the nickel foam was subjected to UV irradiation (BZS250GF-TC, Wuhan Huiwo Technology, Wuhan, China) at wavelengths of 253.7 nm and 184.9 nm, corresponding to photon energies of approximately 472 and 647 kJ·mol^{-1}, respectively. The UV source had a power of 250 W and was positioned 30 mm above the sample surface. Both sides of the foam were irradiated for 10 min each. Under these conditions, the high-energy photons are sufficient to cleave most molecular bonds. Organic contaminants adsorbed on the foam surface were broken, oxidized, or photo-aged by the UV irradiation and subsequently decomposed into volatile species such as CO_2 and H_2O, which were removed from the surface. As a result, the surface cleanliness of the nickel foam was greatly improved,

allowing residual organic films to be reduced to near the monolayer level and significantly increasing the number of electrochemically active sites available for subsequent nickel electrodeposition.

After UV cleaning, the electroplating experiments were performed using a self-made electroplating equipment. In the single-stage electroplating, 200 mL of the primary plating baths were heated to designed temperature (50, 60 and 70 °C), and the pretreated substrate (nickel foam or stainless steel) and pure nickel plates were connected to the cathode and anode of the power supply, respectively. With a magnetic stirring speed of 550–750 rpm, electroplating was carried out at a voltage of 0.08 V cm^{-2} and a current density of 0.21 A cm^{-2} (constant current mode). After electroplating, the samples were rinsed with deionized water and dried for subsequent second-stage electroplating. The operation of the two-stage electroplating was similar to the single-stage electroplating, while the secondary electroplating solution and the substrate after single-stage electroplating were selected as the plating solution and the cathode, respectively. In addition, the voltage and current density for the second-stage electroplating were 0.31 V cm^{-2} and 0.21 A cm^{-2}, respectively, with the electroplating time and temperature being the same as those for the first stage.

2.3. Mechanical and Electrochemical Characterization Methods

X-ray diffraction (XRD) analysis of electroplated samples was performed using a PANalytical X-pert Powder diffractometer (Malvern Panalytical, Almelo, The Netherlands) with Cu Kα radiation (λ = 1.5406 Å), a scanning range (2θ) of 10–80°, a scanning rate of 5° min^{-1}, an operating voltage of 40 kV and a current of 40 mA. Microstructure analysis was conducted using a Zeiss Sigma 360 field-emission scanning electron microscope (FE-SEM, Carl Zeiss AG, Oberkochen, Germany) with an accelerating voltage of 5–20 kV. Tribological property testing was carried out on a Bruker UMT-2 multifunctional tribometer (Bruker, San Jose, CA, USA) under the following experimental conditions with GCr15 bearing steel ball (Φ4 mm) as the counterpart, a normal load of 2 N, reciprocating circular motion (radius 2.5 mm), sliding speed of 300 rpm, test duration of 30 min, and ambient room temperature conditions (relative humidity 40–60%), with the friction coefficient being recorded in real time by the system software. Mechanical property testing was conducted using a Wilson Hardness Tukon 2500 microhardness tester (Buehler, Lake Bluff, IL, USA) with a Vickers hardness (HV) test method under a test load of 100 gf and a dwell time of 15 s. Electrochemical performance evaluation was performed using a Princeton Versa STAT 4 electrochemical workstation (Princeton Applied Research, Oak Ridge, TN, USA) with a 3.5 wt% NaCl solution (25 ± 1 °C) as the electrolyte in a three-electrode system with the test sample (exposed area 1 cm^2) as the working electrode and a Ag/AgCl reference electrode and a Pt counter electrode. Samples were immersed in the electrolyte for 30 min to reach steady-state conditions before testing. Open circuit potential measurement was followed by Tafel polarization and electrochemical impedance spectroscopy (EIS) tests with EIS conducted over a frequency range of 100 kHz–10 mHz using an AC perturbation amplitude of 10 mV. All experiments were performed using independently prepared samples, and each test was repeated at least three times.

3. Results and Discussion

3.1. Compositions and Morphology of Electroplated Nickel Coatings

The pre-experiment was conducted using 304 stainless steel as the substrate to investigate the compositions of electroplating coatings. Figure 1a,b present the XRD patterns of nickel-plated stainless steel samples after single-stage and two-stage electroplating at constant electroplating temperature (60 °C) for various electroplating time. It demonstrates

that after nickel plating treatment, the characteristic diffraction peaks of the 304 stainless steel substrate completely disappeared and are replaced by diffraction peaks corresponding to the (111), (200), and (220) crystal planes of metallic nickel (PDF#04-0850), which indicates that the plated coating completely covers the substrate. It is noted that the single-stage electroplated coatings exhibits obvious preferred orientation along the (220) plane, while the two-stage electroplating process alters the crystalline orientation characteristics of the coating. The (220) plane diffraction intensity of the coating markedly decreases, while the (111) plane diffraction peak significantly intensified. With the increase in electroplating time, the diffraction peak intensities of both (200) and (220) planes show a gradual weakening trend, which indicates a significant transition in coating crystal growth orientation from high-index planes (220) toward the more stable (111) direction. Such preferred orientation changes are possibly associated with reduced internal stress and improved structural stability in the coatings. In the face-centered cubic nickel coatings, the enhanced diffraction intensity of the (111) plane as the close-packed plane indicates that more grains are aligned parallel to this low-energy plane on the substrate surface, forming a denser atomic arrangement. This structural evolution significantly improves coating properties. The (111) orientation reduces surface energy to enhance corrosion resistance, while the formation of close-packed planes increases mechanical and thermal stability. The observed weakening of (220) diffraction and strengthening of (111) peaks experimentally confirms that the two-stage electroplating process effectively controls crystal growth orientation to produce superior nickel coatings. Figure 1c presents XRD patterns of nickel coatings after two-stage electroplated at 8 min under different temperatures. It is seen that when the temperature increases from 50 to 70 °C, the diffraction intensities of both (200) and (220) planes show significant attenuation, and a weak NiO impurity peak emerges at $2\theta = 43°$ at 70 °C. Considering both crystalline integrity and phase purity, 60 °C is determined as the suitable electroplating temperature. XRD testing was conducted on nickel foam and nickel-plated nickel foam (Figure 1d), and the results revealed that the diffraction peaks almost overlapped. This can be attributed to the fact that the coating and the nickel foam are made of nickel.

Based on the electroplating on 304 stainless steel substrates, the single-stage and two-stage electroplating on foam nickel substrates were further conducted at constant temperature of 60 °C, and the effects of different electroplating time (3, 8, and 10 min) on morphology of coatings were systematically investigated. Figure 2a–c show the actual pictures of nickel-plated nickel foam after single-stage electroplating processes. It is observed that the right portions of the nickel-plated nickel foam display areas treated with single-stage nickel plating, while the left portions show the original sections without electroplating. The single-stage electroplating process achieved complete nickel layer coverage on the foam nickel substrate, which builds a foundation for subsequent two-stage electroplating. Figure 2d–f present the actual pictures of samples after two-stage electroplating. It reveals that there are complete and dense coatings with characteristic silvery-white metallic luster on the surface of nickel foam. It should also be noted that after single-stage and two-stage electroplating at 60 °C for 10 min, “burnt” deposits were observed on the sample surface. These deposits may be caused by the relatively long electrodeposition time, which leads to a locally high current density. Figure 3a–c present the morphological characteristics of nickel foam subjected to a two-stage electroplating process following 10 min of UV cleaning pretreatment. The results demonstrate that optimal nickel coating with excellent brightness and uniformity can be achieved under the following conditions: 10 min UV pretreatment, electroplating temperature maintained at 60 °C, and an electroplating duration of 8 min.

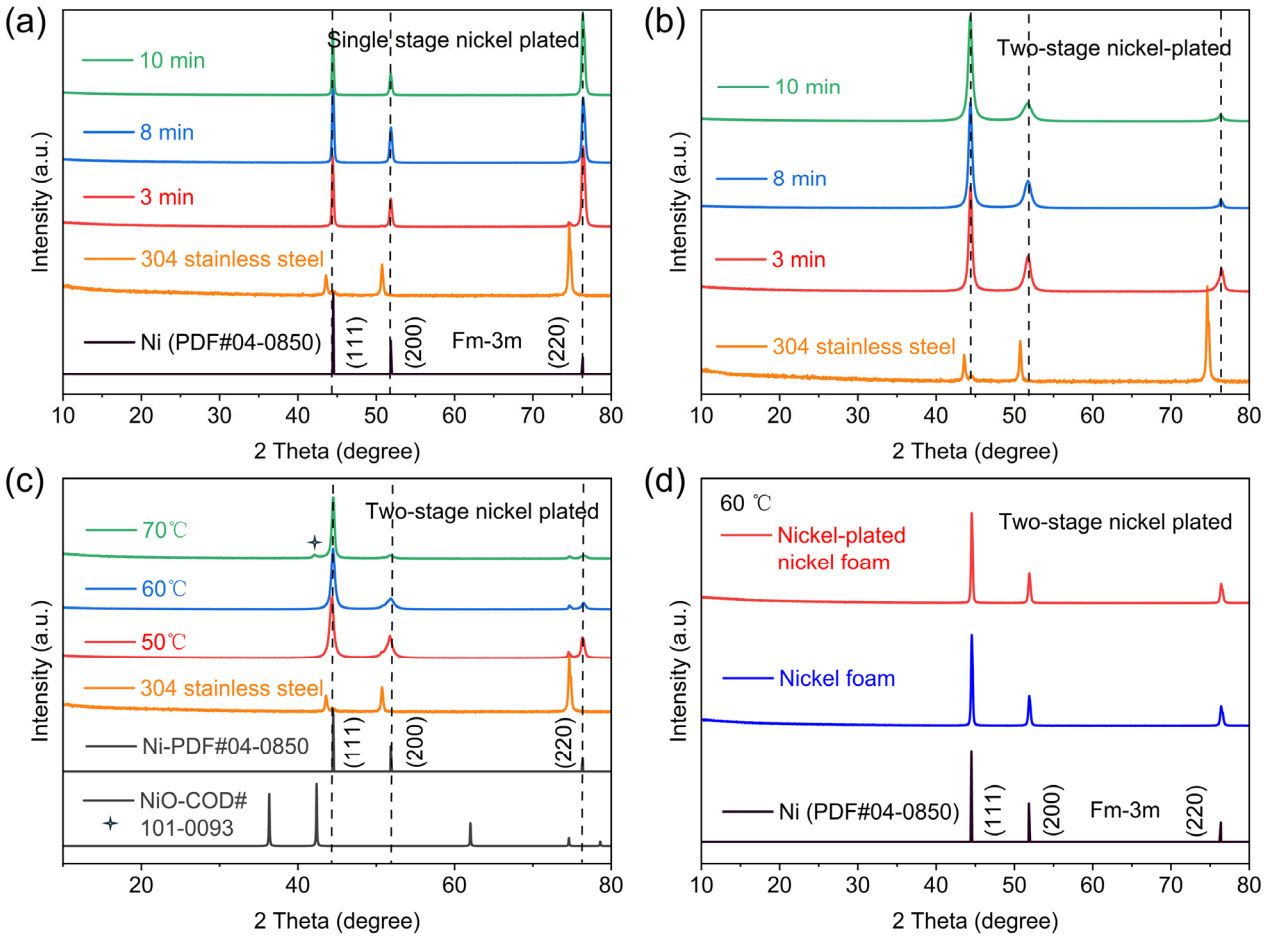


Figure 1. XRD patterns of nickel-plated 304 stainless steel samples: (**a**) XRD patterns of single-stage nickel-plated coatings with different electroplating time (60 °C); (**b**) XRD patterns of two-stage nickel-plated coatings with different electroplating time (60 °C); (**c**) XRD patterns of two-stage nickel plating coatings at different temperatures for 8 min. (**d**) XRD patterns of two-stage nickel-plated coatings on nickel foam, which were plated at 60 °C for 8 min.

Figure 4a–c present the microstructural evolution of nickel-plated nickel foam after single-stage electroplating at 60 °C for 3, 8 and 10 min. It reveals that the sample after single-stage electroplating for 3 min exhibits loose grain distribution, while an enhanced grain packing density is achieved when the electroplating time increases to 8 min. When the electroplating time reaches 10 min, the grains develop into pyramidal structures but show abnormal coarsening with diameters up to 3 μm, which indicates that prolonged plating time provides a sustained growth driving force for grains, and electrode interface free energy promotes preferential grain orientation. By comparison, the sample after single-stage electroplating for 8 min possesses optimal grain size and density, which builds an ideal basis for subsequent two-stage electroplating. Figure 4d–f illustrate the microstructural evolution of nickel-plated nickel foam after two-stage electroplating at 60 °C for 3, 8 and 10 min. It is seen that the sample after two-stage electroplating for 3 min displays sparse nickel crystal distribution, while uniform nickel crystals with the size of 500 nm formed for the one after two-stage electroplating for 8 min. The sample after two-stage electroplating for 10 min showed dense and homogeneous coating structure and higher crystallinity and crystal size. This morphological evolution demonstrates that electroplating time critically influences the growth of nickel crystals, and appropriately extending the electroplating time facilitates the formation of coatings with structural uniformity.

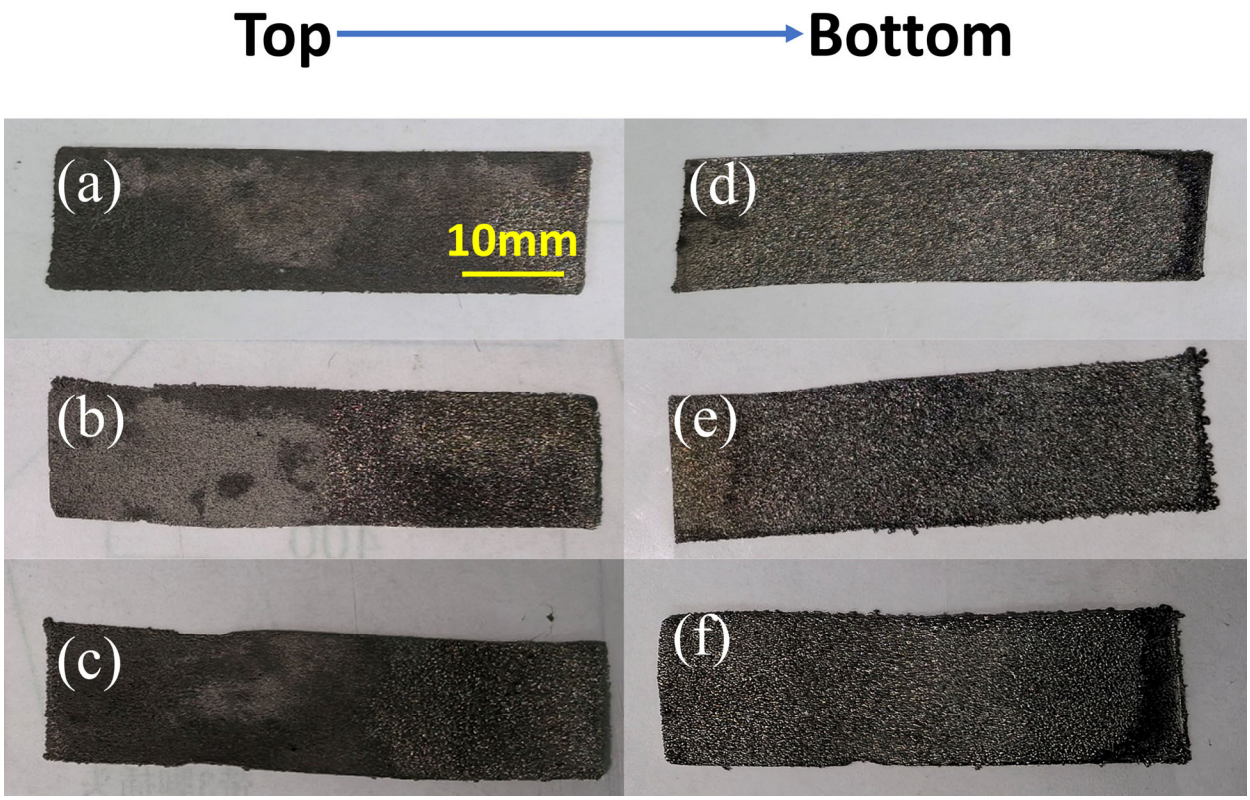


Figure 2. Pictures of nickel foam samples: (**a**–**c**) Pictures of nickel foam samples after single-stage electroplating at 60 °C for 3, 8 and 10 min, (**d**–**f**) pictures of nickel foam samples after two-stage electroplating at 60 °C for 3, 8 and 10 min. The left side of the coating is the non-plated area, and the right side is the plated area.

Figure 5a–f show the regulation of electroplating temperature on the microstructure of nickel-plated nickel foam after two-stage electroplating. It is noted that the electroplating temperature has an important role on the deposition behavior of nickel coating on the surface of nickel foam. At 50 °C, discontinuous island-like nickel occurs on the framework of nickel foam. When the temperature increases to 60 °C, the nickel deposits exhibit uniform and dense morphology with homogeneous crystal size distribution. Further increasing the temperature to 70 °C will produce an excessive deposition rate, resulting in high thickness and crystal coarsening of coating. Comprehensive morphological analysis and crystallographic characterization reveal that the sample electroplated at 60 °C for 8 min demonstrates the most favorable overall performance with uniform crystal size (approximately 500 nm), packing density, and defect-free structure. It indicates that the suitable electroplating temperature is 60 °C, at which we can avoid the formation of loose structure caused by insufficient crystal formation at 50 °C and prevent excessive crystal growth at 70 °C. In summary, 10 min of UV pretreatment for nickel foam and the 8 min of electroplating time and 60 °C of electroplating temperature of two-stage electroplating establishes a reliable process window for obtaining high-quality nickel coatings on the nickel foams.

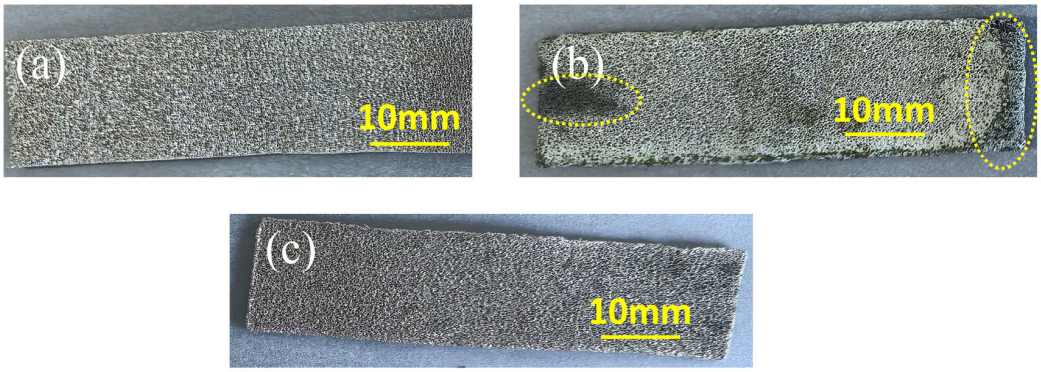


Figure 3. (**a**) Pictures of nickel foam before electroplating, (**b**) picture of nickel foam after electroplating for 8 min at 60 °C without UV cleaning (The yellow circles mark the "burnt" deposits), (**c**) picture of nickel foam after electroplating for 8 min at 60 °C with UV cleaning.

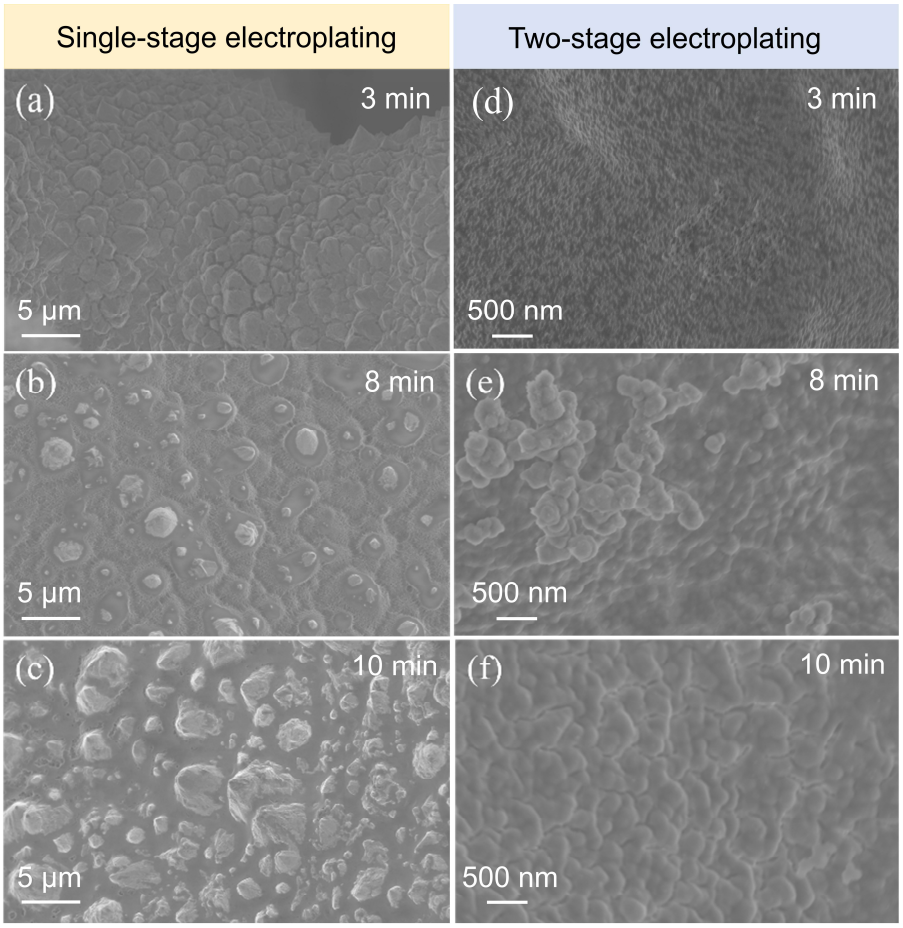


Figure 4. (**a**–**c**) SEM images of nickel-plated nickel foam after single-stage electroplating at 60 °C for 3, 8, and 10 min, (**d**–**f**) SEM images of nickel-plated nickel foam after two-stage electroplating at 60 °C for 3, 8, and 10 min.

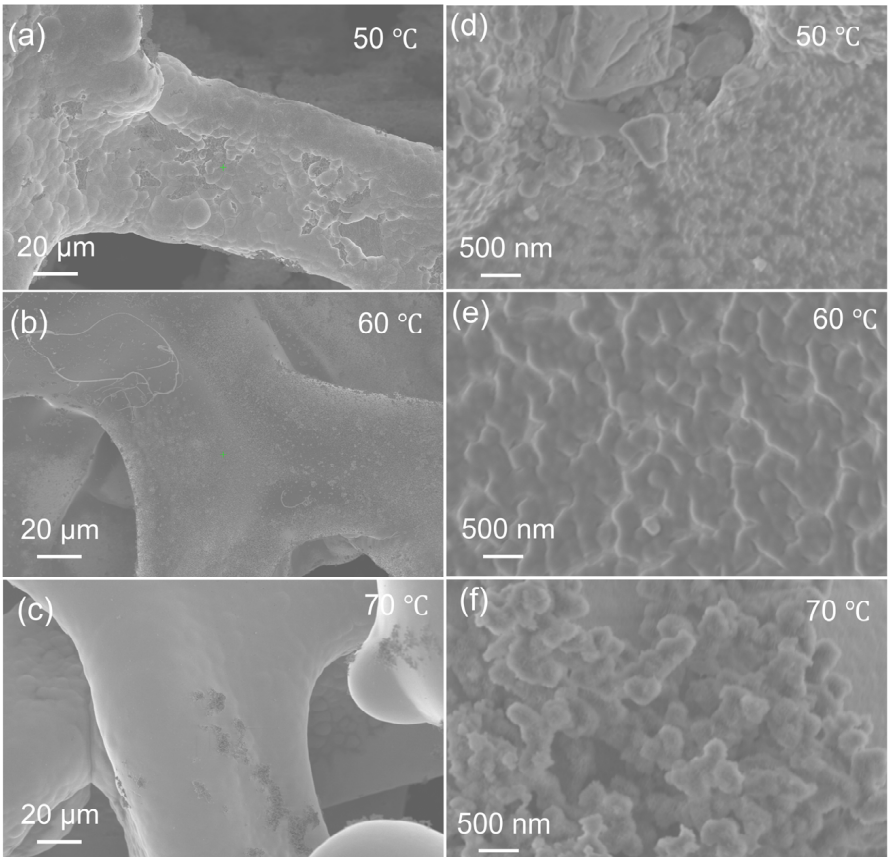


Figure 5. SEM images of nickel-plated nickel foam after two-stage electroplating at 50 (**a**,**d**), 60 (**b**,**e**) and 70 °C (**c**,**f**) for 8 min.

3.2. Mechanical Properties of Nickel-Plated Nickel Foam

The mechanical properties of foam nickel are very important in determining whether it can be used for sand control screens, especially the hardness, which is a key indicator to evaluate the wear resistance of foam nickel. In this study, Vickers hardness measurements were conducted on both nickel-plated nickel foam after two-stage electroplating under optimal conditions and pristine nickel foam samples, as shown in Figure 6. It demonstrates that the nickel-plated nickel foam exhibits an average hardness of 3571 N/mm^2, while the pristine nickel foam only has average hardness of 747 N/mm^2, indicating that two-stage electroplating increases the hardness of foam nickel by six times and significantly enhances the wear resistance of foam nickel. The scatter in microhardness values of the nickel-plated foam is primarily attributed to its localized structural heterogeneity. The measured hardness is highly dependent on the indentation site: indentations on solid struts reflect the intrinsic strength of the nickel material, whereas those near strut edges or over pores involve local bending or buckling rather than pure plastic deformation. This combination of material- and structure-dominated responses, together with the stochastic distribution of pores, accounts for the observed variation. Consequently, the scatter is not an experimental error but a meaningful representation of the foam's microstructural characteristics. Higher hardness values capture the intrinsic strength of the nickel struts, while lower values reflect the local structural compliance and energy-absorption capacity of the pores. Such site-specific measurements provide a dual-scale insight unattainable by bulk testing, effectively decoupling the contributions of the constituent material from the overall foam architecture.

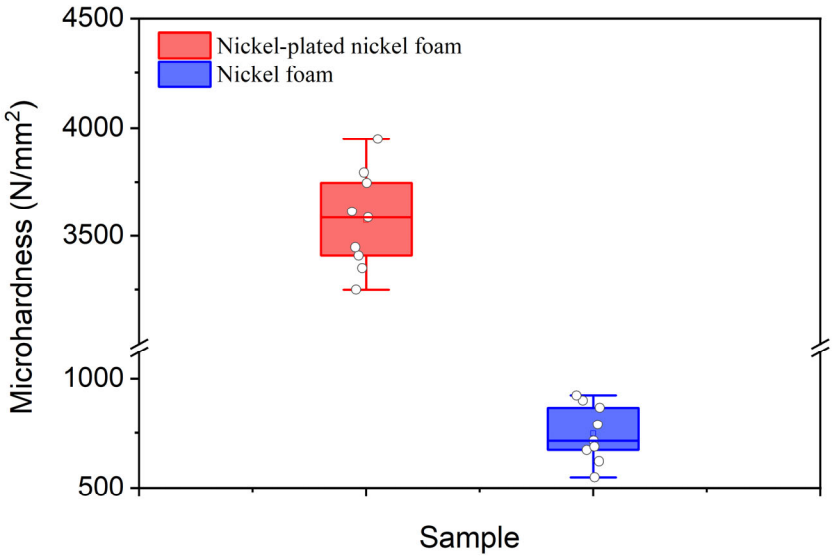


Figure 6. Box plots comparing the hardness of nickel-plated nickel foam under the optimal process conditions (10 min of UV pretreatment, electroplating temperature of 60 °C, and electroplating time of 8 min) and the original nickel foam.

Combined with scanning electron microscopy (SEM) image analysis, it is evident that under optimal processing conditions, the dense nickel-plated coating uniformly and tightly covers the nickel foam framework. This microstructural modification significantly enhances the hardness properties of the nickel foam, endowing it with superior characteristics that meet the requirements for petroleum sand control materials, thereby providing an improved material option for sand control engineering applications.

3.3. Electrochemical Corrosion Resistance of Nickel-Plated Nickel Foam

The chemical stability of nickel foam determines its service life in sand control screens, while the electrochemical corrosion resistance is a key indicator to chemical stability of nickel foam. The polarization curve and fitted curve of the Tafel region of nickel-plated nickel foam under the optimal process conditions (10 min of UV pretreatment, 60 °C of electroplating temperature, and 8 min of electroplating time) and original nickel foam were characterized to evaluate the electrochemical corrosion resistance of nickel foam, as shown in Figure 7. It is observed that the pristine nickel foam exhibits a corrosion potential of -0.92 (± 0.07) V and a corrosion current of 7.00 (± 4.86) $\times$ 10^{-5} A cm^{-2}, whereas the nickel-plated nickel foam shows a negative shift in corrosion potential to -0.97 (± 0.06) V and an increased corrosion current of 2.00 (± 0.48) $\times$ 10^{-4} A cm^{-2}. The Tafel slope of the original nickel foam is 0.260 (± 0.002) V/dec, while that of the nickel-plated foam nickel is 0.308 (± 0.036) V/dec. Corrosion inhibitors can form an adsorption film on the metal surface. By altering the activation energy of the electrode reaction, they effectively slow down the corrosion rate of the metal. As for coating protection, a protective film is applied to the metal surface. This film acts like a barrier, creating a physical shield that isolates the metal from external corrosive media, significantly enhancing the protective effect [30]. The results indicate that the nickel plating treatment significantly increases the corrosion current of the foam nickel. Generally, a higher corrosion current implies poor corrosion resistance of the nickel coating. This might be attributed to the presence of an oxide layer on the surface of the initial nickel foam. Although the nickel metal coating enhances the mechanical strength of the foam nickel, the corrosion current of the metallic nickel layer is higher compared to that of the oxide layer on the foam nickel. Even though the corrosion resistance of the nickel-plated layer itself is relatively weak, in the entire foam structure system, it serves as a shield against the external environment. Moreover, in a corrosive

environment, the nickel-plated layer corrodes preferentially. By sacrificing itself, it provides protection for the foam structure, effectively prolonging the overall service life of the foam structure and enhancing its overall corrosion resistance.

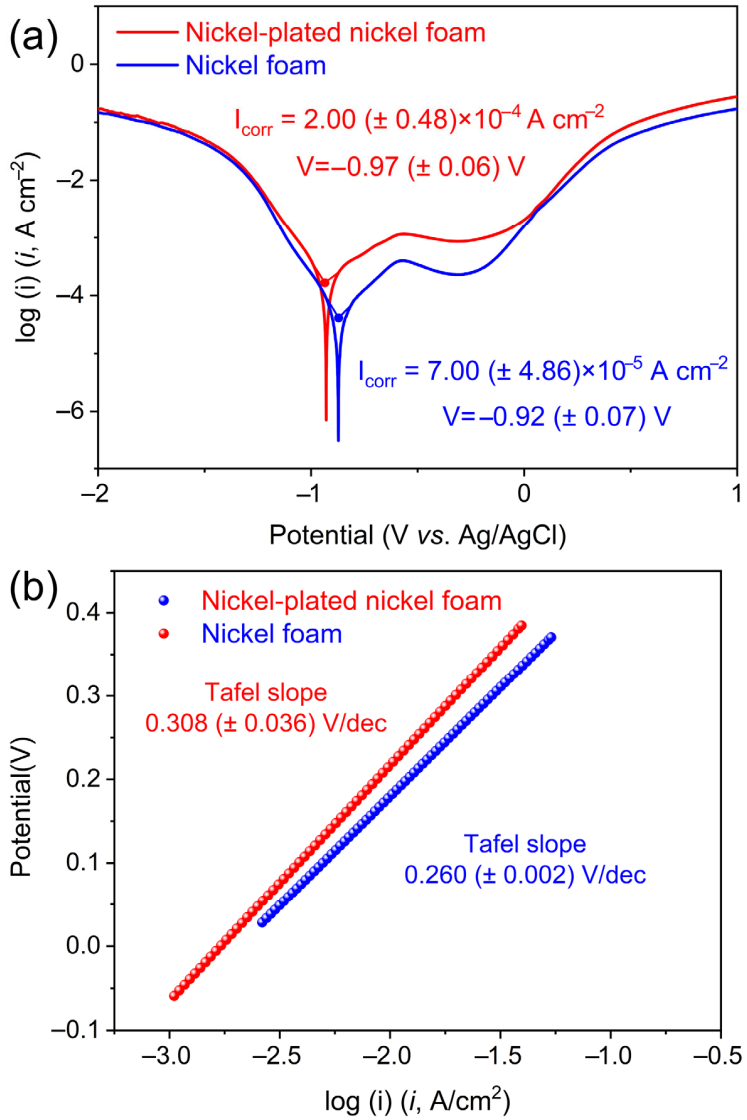


Figure 7. (**a**) Polarization curve and (**b**) fitted curve of the Tafel region of nickel-plated nickel foam under the optimal process conditions (10 min of UV pretreatment, 60 °C of electroplating temperature, and 8 min of electroplating time) and original nickel foam.

Figure 8 compares the electrochemical impedance spectroscopy (EIS) results of pristine nickel foam and nickel-plated nickel foam. For Nickel-plated nickel foam, the ohmic resistance R_s was approximately 3.9 Ω, while the charge-transfer resistance R_{ct} reached 4100 Ω. In contrast, Nickel foam exhibited an R_s of about 4.0 Ω and a significantly lower R_{ct} of roughly 1500 Ω. The experimental data show that the nickel plating treatment significantly reduces the charge-transfer resistance of the material, which is manifested as a significantly smaller semicircle diameter of the plated sample in the Nyquist plot. This phenomenon suggests that the nickel coating enhances conductivity through the following mechanisms: (1) Filling the microdefects and pores on the surface of the skeleton, thereby reducing interfacial scattering during electron transport. (2) Forming a continuous metallic conductive network, effectively lowering the contact resistance. (3) Covering the surface oxide layers and non-conductive phases, substantially decreasing the grain boundary resistance. In addition, the dense nickel coating can act as both a sacrificial layer and a

physical barrier, preventing the foam substrate from direct contact with corrosive media and greatly extending the service life of the nickel foam screen.

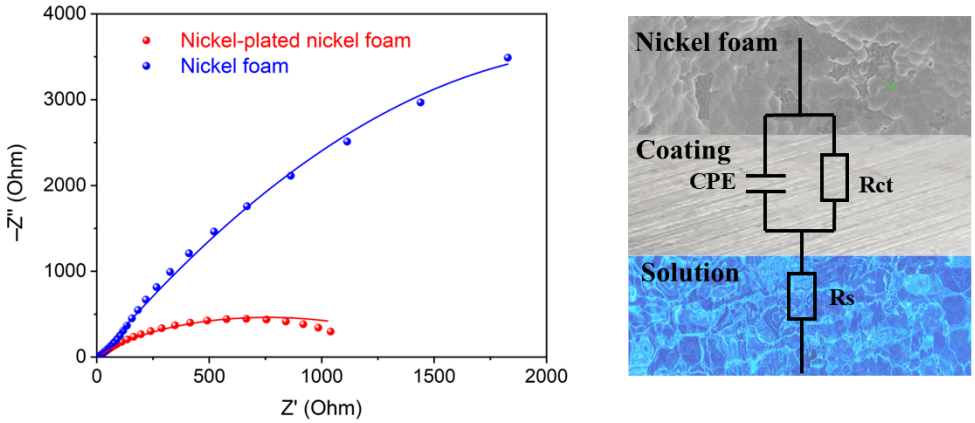


Figure 8. Electrochemical impedance spectra and equivalent circuit diagrams of nickel-plated nickel foam under the optimal process conditions (10 min of UV pretreatment, electroplating temperature of 60 °C, and electroplating time of 8 min) and the original nickel foam.

3.4. Friction Resistance of Nickel-Plated Nickel Foam

In petroleum sand control applications, the coefficient of friction represents a critical parameter of substantial significance. A higher friction coefficient indicates that the material can more effectively capture sand particles entrained in petroleum flow during production, thereby providing more reliable protection for sand control operations. Figure 9 displays the friction curves of both pristine nickel foam and nickel-plated nickel foam samples after two-stage electroplating under optimal conditions (10 min of UV pretreatment, 60 °C of electroplating temperature and 8 min of electroplating time). It demonstrates that during the initial 3 min of the friction test, both samples exhibit significant fluctuations in their friction coefficients. As the test progressed beyond this period, the friction coefficients gradually stabilize. Comparative analysis reveals that the nickel-plated nickel foam shows a substantially higher friction coefficient than pristine nickel foam. Furthermore, the nickel-plated nickel foam maintains more stable friction coefficient value throughout the entire testing duration, which clearly indicates that the nickel-plated layer significantly enhances the friction resistance properties of nickel foam.

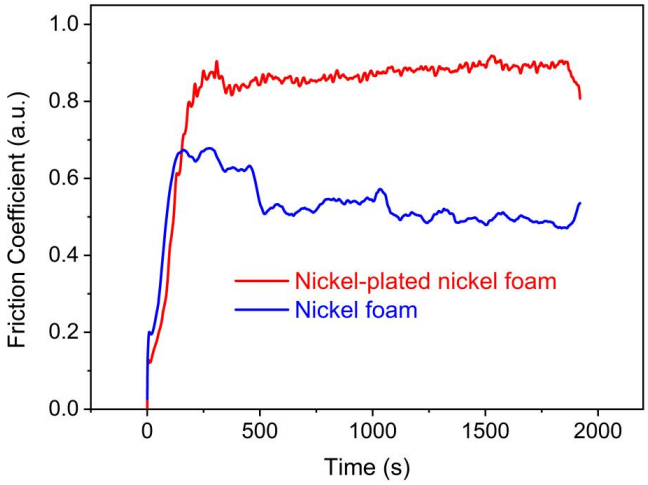


Figure 9. The time-coefficient of friction curves of nickel-plated nickel foam under the optimal process conditions (10 min of UV pretreatment, 60 °C of electroplating temperature, and 8 min of electroplating time) and original nickel foam.

4. Conclusions

The electroplating was successfully used to plate nickel coating on the nickel foam, and the process parameters were optimized. The compositions, morphology and microstructure and of single-stage electroplating and two-stage electroplating under different electroplating time and temperature were investigated, and the properties of nickel-plated nickel foam and original nickel foam were compared. The electroplating time and temperature and UV cleaning pretreatment have an important role on the coating formation, and the optimal electroplating conditions are 10 min of UV pretreatment, 60 °C of electroplating temperature, and 8 min of electroplating time for two-stage electroplating. The as-prepared nickel layer displays virtually no pinholes, plating spots and impurity deposition, presenting a bright surface with strong adhesion. The nickel-plated coating maintains complete crystalline structure, significantly enhancing both stability and bonding strength. The hardness of nickel-plated nickel foam reached nearly six times than that of pristine nickel foam. Furthermore, the nickel-plated nickel foam demonstrates superior chemical corrosion resistance and significantly higher friction coefficient compared to original nickel foam. The nickel-plated nickel foam with precise regulation of filter mesh pore size and surface characteristics enables more accurate sand control performance, and enhances its corrosion and erosion resistance in harsh well conditions, substantially extending service life and reducing workover operations. The research outcomes not only contribute to improved efficiency and reliability in petroleum production sand control processes but also provide a solid foundation for further development and optimization of related materials, with promising prospects for widespread application in the petroleum industry to drive continuous technological advancement.

Author Contributions: Writing—original draft, W.W. (Wenbo Wang) and X.L.; Methodology, W.W. (Wenbo Wang), W.W. (Wen Wen) and H.Y.; Validation, X.L. and Z.P.; Project administration, Z.P., W.W. (Wen Wen) and H.Y.; Data curation, W.W. (Wenbo Wang); Conceptualization, S.B.; Supervision, Z.P. and S.B.; Writing—review and editing, X.W. and X.G.; Funding acquisition, X.W. and X.G. All authors have read and agreed to the published version of the manuscript.

Funding: This research was financially supported by the Key Science and Technology Projects for Basic and Prospective Research of CNPC (No.: 2023ZZ11).

Data Availability Statement: The original contributions presented in this study are included in the article. Further inquiries can be directed to the corresponding authors.

Conflicts of Interest: Authors Shengchi Bai, Wen Wen, Huidi Yu and Xiaoqi Wang were employed by Research Institute of Petroleum Exploration & Development of China National Petroleum Corporation (RIPED). The remaining authors declare that the research was conducted in the absence of any commercial or financial relationships that could be construed as a potential conflict of interest.

References

1. Deng, F.C.; Feng, Y.C.; Yan, C.L.; Lin, H.; Gong, N.; Wang, J. Experimental investigation of factors affecting gravel pack efficiency for thermal recovery wells in Bohai Bay, China. *J. Pet. Sci. Eng.* **2017**, *156*, 835–844. [CrossRef]
2. Li, X.R.; Feng, Y.C.; Gray, K.E. A hydro-mechanical sand erosion model for sand production simulation. *J. Pet. Sci. Eng.* **2018**, *166*, 208–224. [CrossRef]
3. Dong, C.Y.; Gao, K.G.; Dong, S.X.; Shang, X.S.; Wu, Y.X.; Zhong, Y.X. A new integrated method for comprehensive performance of mechanical sand control screens testing and evaluation. *J. Pet. Sci. Eng.* **2017**, *158*, 775–783. [CrossRef]
4. Barbour, M.E.; Lussi, A.; Shellis, R.P. Screening and prediction of erosive potential. *Caries Res.* **2011**, *45*, 24–32. [CrossRef] [PubMed]
5. Dong, C.; Cui, M.; Peng, J.; Wang, P.; Jiang, W.; Zhang, D.; Zhang, Q.; Fu, J. Experimental study on selection of mechanical screens and sand retention precision design for horizontal wells in a gas field. *J. China Univ. Petroleum. Ed. Natrual Sci.* **2015**, *39*, 104–109.
6. Xiao, Y.B.; Huang, J.J.; He, F.J.; Yang, J. Application of iron-nickel-tungsten alloy plating to cylinder liner. *Electroplat. Finish.* **2011**, *30*, 6–9.

7. Hou, D.; Shi, T.; Zeng, D.; Wang, Q.; Liu, W. Coating microstructure characteristics and corrosion resistance of electroplating W alloy. *Mater. Rev.* **2012**, *26*, 12–15.
8. Chen, S.; Liu, L.; Li, J.; Huang, S.; Tang, C.; Zhong, C. Recent progress in electrodeposition of Ni and Ni-based alloys. *Mater. Rev.* **2012**, *26*, 110–115.
9. Wang, Z.; Peng, H.; Wang, C.; Chen, Z. Processes and formulations for multi-layered nickel electroplating. *Electroplat. Finish.* **2015**, *34*, 940–952.
10. Ge, Y.; Zhao, C.; Zhan, Z.; Zhang, Q.; Sun, Z. Research progress of wear-resistant electrodeposited nickel-based composite coatings. *Electroplat. Finish.* **2020**, *39*, 1523–1527.
11. Boonyongmaneerat, Y.; Sukjamsri, C.; Sahapatsombut, U.; Saenapitak, S.; Sukkasi, S. Investigation of electrodeposited Ni-based coatings for biodiesel storage. *Appl. Energy* **2011**, *88*, 909–913. [CrossRef]
12. Yao, J.; He, X.; Chen, Y.; Tang, X.; Peng, S. Electroless nickel pre-plating as a substitute for palladium activation before electroless nickel plating on copper patterns of printed circuit boards. *Electroplat. Finish.* **2018**, *37*, 160–164.
13. Maniam, K.K.; Paul, S. Progress in electrodeposition of zinc and zinc nickel alloys using ionic liquids. *Appl. Sci.* **2020**, *10*, 5321. [CrossRef]
14. Jesmani, S.M.; Aberi, M.; Banasaz, H.; Mirzamohammadi, S. Investigation of licorice extract as a green additive on microstructure, hardness, and wear behavior of electrodeposited nickel coatings. *Sci. Rep.* **2025**, *16*, 3023. [CrossRef]
15. Archard, J.F. Contact and Rubbing of Flat Surfaces. *J. Appl. Phys.* **1953**, *24*, 981–988. [CrossRef]
16. Tong, H.; Han, W.; Zhang, Y.; Lin, Z.; Wei, S.; Xu, B. Application and prospect of surface engineering technology in petroleum and petrochemical pipelines. *Surf. Technol.* **2017**, *46*, 195–201.
17. Safavi, M.S.; Walsh, F.C. The electrodeposition of particle-metal matrix composite coatings to meet tribological and corrosion challenges. *Adv. Colloid Interface Sci.* **2025**, *343*, 103584. [CrossRef]
18. Zhang, X.F.; Gong, X.B.; Wang, D.S.; Liu, S.P.; Zhang, Y.X. Stimuli-responsive micro/nanocontainers for multifunctional anticorrosive coatings: Design, mechanism, and applications. *Prog. Org. Coat.* **2026**, *210*, 109712. [CrossRef]
19. Zhao, X.Y.; Hou, Y.Y.; Ren, Z.C.; Liu, M.M. Progress of electrodeposition of nickel-based anticorrosive wear-resistant coatings in deep eutectic solvents. *J. Electrochem. Soc.* **2025**, *172*, 102505. [CrossRef]
20. Shin, E.G.; Rehman, A.U.; Lee, S.H.; Lee, S.H. Nickel electroless plating: Adhesion analysis for mono-type crystalline silicon solar cells. *J. Nanosci. Nanotechnol.* **2015**, *15*, 7823–7827. [CrossRef]
21. He, X.H.; Gu, Y.Q. Production process control of barrel nickel plating of steel battery shell. *Electroplat. Finish.* **2007**, *26*, 30–32.
22. Wu, Y.; Zhang, Z.D.; Leng, J.; Gao, C.Z.; Huang, G.; Qi, F.D.; Lu, T.C.; Shi, Q.W. Supercritical oxidation resistance of double-layer aluminized coating on nickel alloy prepared by pack cementation aluminizing. *Surf. Coat. Technol.* **2025**, *497*, 131728. [CrossRef]
23. Yang, X.H.; Zhang, X.M.; Ming, P.M.; Xiao, Y.P.; Guo, X.Y. Current trends and future prospects of electrodeposition technology for the preparation of heterogeneous structural materials. *J. Manuf. Process.* **2025**, *134*, 29–59. [CrossRef]
24. Sreekumar, R.; Nair, A.S.; Sreejakumari, S.S. Recent trends and developments in two-dimensional materials based electrodeposited nickel nanocomposite coatings. *FlatChem* **2022**, *36*, 100434. [CrossRef]
25. Gao, M.Y.; Pei, Z.L.; Gong, J.; Song, G.H. The improved wear resistance of Ni-based composite coatings by the synergistic effect of diamond and self-lubricating particles. *Colloids Surf. A Physicochem. Eng. Asp.* **2026**, *730*, 138983. [CrossRef]
26. Yanai, T.; Tashiro, M.; Shiraki, K.; Yamashita, A.; Nakano, M.; Fukunaga, H. Preparation of Ni Films using Solid/Liquid Hybrid Electroplating Method. *J. Magn.* **2025**, *30*, 483–487. [CrossRef]
27. Shi, Y.P.; Sun, L.; Wang, J.; Zhang, H.T.; Huang, C.H. Optimizing electroless Ni-P coating on the Inner wall of 304 stainless steel pipes: Control of plating solution flow rate for enhanced microstructural uniformity and corrosion resistance. *Metall. Mater. Trans. A-Phys. Metall. Mater. Sci.* **2025**, *56*, 2129–2150. [CrossRef]
28. Min, S.K.; Jang, I.C.; Kim, M.; Kim, K.B. Electrochemical corrosion resistance evaluation of Zn-Ni alloy electroplating process in zincate bath. *Appl. Sci. Converg. Technol.* **2024**, *33*, 36–40. [CrossRef]
29. Guerrero, J.D.M.; Satpathy, B.; Prasad, P.S.; Das, S.; Das, K. Electrodeposition process optimization by response surface methodologies to obtain high-corrosion resistant Zn-Ni coatings. *Surf. Coat. Technol.* **2024**, *479*, 130561. [CrossRef]
30. Khormali, A. Using a new mixture of reagents for effective inhibition of corrosion and salt precipitation in the petroleum industry. *J. Chem. Pet. Eng.* **2021**, *55*, 257–276.

Disclaimer/Publisher's Note: The statements, opinions and data contained in all publications are solely those of the individual author(s) and contributor(s) and not of MDPI and/or the editor(s). MDPI and/or the editor(s) disclaim responsibility for any injury to people or property resulting from any ideas, methods, instructions or products referred to in the content.